



Sludge retention time impacts on polyhydroxyalkanoate productivity in uncoupled storage/growth processes

Mariana Matos^{a,b}, Rafaela A.P. Cruz^{a,b}, Pedro Cardoso^a, Fernando Silva^{a,b}, Elisabete B. Freitas^{a,b}, Gilda Carvalho^{a,1}, Maria A.M. Reis^{a,b,*}

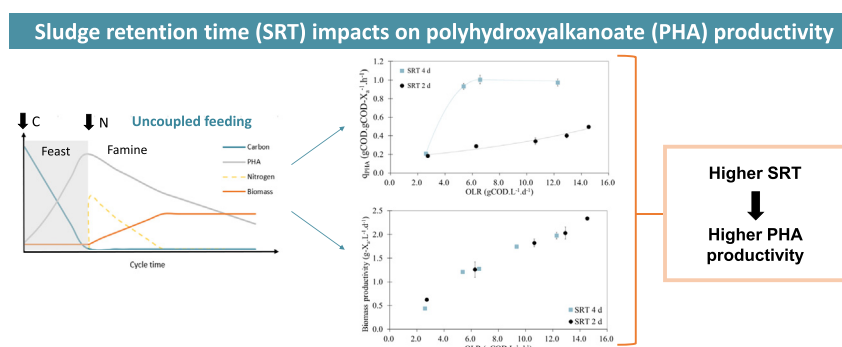
^a UCIBIO – Applied Molecular Biosciences Unit, Department of Chemistry, School of Science and Technology, NOVA University Lisbon, 2819-516 Caparica, Portugal

^b Associate Laboratory i4HB – Institute for Health and Bioeconomy, School of Science and Technology, NOVA University Lisbon, 2819-516 Caparica, Portugal

HIGHLIGHTS

- Pilot scale polyhydroxyalkanoate production with uncoupled carbon/nitrogen feeding.
- Similar biomass volumetric productivities for different sludge retention times.
- Lower sludge retention time favours growth rate and yield.
- PHA storage yield directly linked with relative abundance of putative PHA-storers.
- Higher sludge retention time led to higher storage kinetics/accumulation capacity.

GRAPHICAL ABSTRACT



ARTICLE INFO

Article history:

Received 14 May 2021

Received in revised form 16 July 2021

Accepted 27 July 2021

Available online 30 July 2021

Editor: Daniel CW Tsang

Keywords:

Polyhydroxyalkanoates (PHAs)
Mixed microbial cultures (MMCs)
Pilot-scale
Fruit waste

ABSTRACT

The process involving mixed microbial cultures (MMCs) and waste-based substrates emerged as an alternative solution to reduce the market price of polyhydroxyalkanoates (PHAs). The selection of an efficient MMC that displays a significant PHA accumulation potential and a high growth rate is considered a key factor for the MMC PHA production feasibility. This study used a pilot plant to investigate the dynamics of growth vs storage in a mixed culture fed with fermented fruit waste under uncoupled carbon and nitrogen feeding. Varying sludge retention times (SRTs) (2 and 4 d) and organic loading rates (OLRs) (from 2.6 to 14.5 $gCOD \cdot L^{-1} \cdot d^{-1}$) were imposed for this purpose. Results showed that, regardless of the OLR imposed, cultures selected at lower SRT grew faster and more efficiently using stored PHA. However, they had inferior specific storage rates and accumulation capacity, resulting in lower PHA productivity. Additionally, the polymer storage yield was independent of the SRT, and was directly linked with the abundance of putative PHA-storers in the MMC. The high PHA productivity ($4.6 \pm 0.3 g \cdot L^{-1} \cdot d^{-1}$) obtained for the culture selected at 4 d of SRT was 80% above that obtained for the lower SRT

Abbreviations: μ_{max} , maximum specific growth rate; 3-HB, 3-hydroxybutyrate; 3-HV, 3-hydroxyvalerate; ADF, aerobic dynamic feeding; C, carbon; COD, chemical oxygen demand; C_{SFP} , concentration of soluble fermentation products on reactor broth; DO, dissolved oxygen; EtOH, ethanol; FISH, fluorescence in situ hybridization; FW, fruit waste; GC, gas chromatography; HAc, acetate; HBut, butyrate; HLaC, lactate; HPLC, high performance liquid chromatography; HPrO, propionate; HRT, hydraulic retention time; HVal, valerate; MMC, mixed microbial cultures; N, nitrogen; OLR, organic load rate; OTU, operational taxonomic unit; PCA, Principal component analysis; PHA, polyhydroxyalkanoates; P_X , biomass volumetric productivity; q_{PHA} , specific PHA storage rate; $-q_{PHA}^{famine}$, maximum specific PHA consumption in the famine phase; $-q_{SFP}$, specific substrate uptake rate; SBR, sequential batch reactor; SEC, size exclusion chromatography; SFP, soluble fermentation products; SRT, sludge retention time; TSS, total suspended solids; UASB, upflow anaerobic sludge blanket; VSS, volatile suspended solids; X_{bi} , active biomass; $Y_{PHA/SFP}$, storage yield; $Y_{X/PHA}$, growth yield on PHA.

* Corresponding author at: UCIBIO – Applied Molecular Biosciences Unit, Department of Chemistry, School of Science and Technology, NOVA University Lisbon, 2819-516 Caparica, Portugal.

E-mail address: amr@fct.unl.pt (M.A.M. Reis).

¹ Present address: Advanced Water Management Centre (AWMC), The University of Queensland, St Lucia, QLD, 4072, Australia

Sludge retention time (SRT)
Organic loading rate (OLR)

tested, underlining the importance of achieving a good balance between culture growth and accumulation capacity to increase the viability of the PHA-producing process from wastes.

© 2021 The Authors. Published by Elsevier B.V. This is an open access article under the CC BY-NC-ND license (<http://creativecommons.org/licenses/by-nc-nd/4.0/>).

1. Introduction

The production of plastics emerged in the 1950s and exponentially increased in the following decades, attaining a massive amount of 368 million metric tons in 2019 (Plastics Europe, 2020). Currently, more than 60% of all produced plastics end up in landfills or in the natural environment, causing serious threats to several ecosystems (Geyer et al., 2017). Polyhydroxyalkanoates (PHAs) are an innovative material with great potential to replace the petroleum-derived plastics due to its biodegradable and thermoplastics properties (Kumar et al., 2020; Mannina et al., 2020). The PHA market size is estimated to increase from 62 million USD in 2020 to 121 million USD by 2025 (Markets and Markets, 2021), being a key polymer in the biodegradable plastic market (European Bioplastics, 2020).

A promising PHA production strategy consists in using open mixed microbial cultures (MMCs) and waste-based feedstocks. This approach effectively reduces both the cost and environmental impact associated to PHA obtained from pure cultures and first-generation biomass (Kumar et al., 2018). The MMC process typically consists of a three stage process: (1) fermentation of the carbon feedstock into a mixture of soluble fermentation products (SFP) that are precursors for PHA biosynthesis; (2) selection of an aerobic community highly enriched in PHA-storing bacteria; and (3) production of PHA using the previously selected culture which is fed with the SFP under growth limiting conditions to reach its maximum PHA capacity (Sabapathy et al., 2020).

The selection of a robust culture with a significant PHA accumulation potential and a high growth rate is considered a key factor for the MMC PHA production success. Indeed, these two parameters have a direct impact on the global PHA productivity of the process (Reis et al., 2011; Valentino et al., 2017), so culture selection is a critical step of the three stage process. A high selective pressure towards the enrichment of PHA-storers can be achieved by applying an aerobic dynamic feeding (ADF) strategy, where alternating periods of feast (carbon excess) and famine (carbon absence) are cyclically established in a sequencing batch reactor (SBR) (De Donno Novelli et al., 2021; Sabapathy et al., 2020). Some waste-based feedstocks contain both carbon (C) and nitrogen (N) sources in sufficient amounts for PHA production and bacterial growth. If the substrate contains both a N source and an external C, culture growth usually starts at the beginning of the feast phase, and can be extended into the famine phase depending on the C/N ratio (Albuquerque et al., 2007; Johnson et al., 2010; Serafim et al., 2004). In this situation, storage and growth occur simultaneously during feast, with competition between the two metabolisms. The long famine phase acts then as a physiological selective pressure, inducing the microbial culture to promote storage rather than growth in the following feast phase (Reis et al., 2011).

More recently, Oliveira et al. (2017) and Silva et al. (2017) proposed to uncouple the availability of C and N while maintaining the feast/famine regime during the selection process. This strategy creates a high selective pressure by separating the storage and growth metabolisms. Under these conditions, PHA is stored during feast and the growth of PHA-storers is favoured over other organisms during famine, due to their ability to grow using the previously stored PHA, in the absence of external C source. While the uncoupled feeding strategy can only be used with feedstocks that are poor in nutrients, this approach was shown to be particularly interesting when operating the process at high organic loading rates (OLRs), since it effectively enhanced the PHA storage response by significantly limiting the growth of flanking populations (Argiz et al., 2021; Campanari et al., 2017; Oliveira et al., 2017).

In addition to the OLR and the feeding strategy, the operational sludge retention time (SRT) is also tightly bound to the competition between storage and growth. The SRT theoretically regulates the age of microbial consortia. It can be assumed that, when feeding the C source coupled to the N source, a lower SRT selects a population with increased specific growth rate and growth yield, thus driving a higher amount of C for growth, and less for PHA storage. Lemos et al. (2008) confirmed this hypothesis, using acetate as the sole C source, obtaining lower storage yields and specific PHA storage rates in the selection reactor for lower sludge ages. However, Johnson et al. (2010), observed that the selection and growth/storage dynamics of a culture fed under coupled C and N and operated at different SRTs was also highly dependent on the kind of limitation the culture is experiencing, i.e., if it selected under nitrogen limiting (N is depleted before C) or carbon limited (N is available during all cycle) conditions. These results do not allow to conclude if the lower storage response usually observed for lower SRTs in the SBR is a result of the higher C demand needed for growth (consequence of metabolism), or if it is actually a limitation of the culture that intrinsically has a lower storage ability (consequence of competitive selection). On the other hand, the impact of SRT on culture selection and on PHA production performance was never assessed with the uncoupled strategy. By uncoupling the two processes, the actual mechanisms driving competition between storage and growth could be clarified.

This work aims to elucidate, for the first time, how the dynamics between growth and storage mechanisms change with the SRT when those two metabolic processes are not competing for the same C source (PHA storage from external C in the feast and growth on internal PHA during famine). This strategy was imposed in two pilot-scale SBRs fed with a real nutrient-deficient feedstock – fruit waste (FW) – which were operated at different SRTs. In addition to the highly selective uncoupled C and N regime, the OLR was increased step-wisely in both SBRs up to levels rarely considered in literature (maximum $14.5 \text{ gCOD.L}^{-1}.\text{d}^{-1}$) and maximum PHA content on biomass was envisaged to enhance the global PHA productivity. This performance parameter has a strong impact in the design of the PHA production process, therefore it is a good indicator to compare the culture efficiency and the process viability under different conditions.

2. Materials and methods

2.1. Experimental set-up and operation of the reactors

A three-stage pilot scale was operated for PHA production using MMCs. The experimental setup used is schematically represented in Fig. 1. The FW was fed to an acidogenic fermenter (step 1), where its organic carbon was converted into a mixture of SFP. This step was followed by a decanting stage, where the resulting SFP stream was clarified to remove the coarse solids facilitating the operation of the subsequent reactors. The refined SFP stream was then fed to the selection reactor (step 2), for the enrichment of a PHA-producing MMC and to a PHA accumulation reactor (step 3), where the previously selected culture was inoculated and fed with the fermented FW until attaining its maximum PHA storage capacity.

2.1.1. Acidogenic fermentation

An upflow anaerobic sludge blanket (UASB) reactor with a working volume of 60 L was operated in continuous mode. For the specific period in which the SFP were collected, the operating conditions were set as

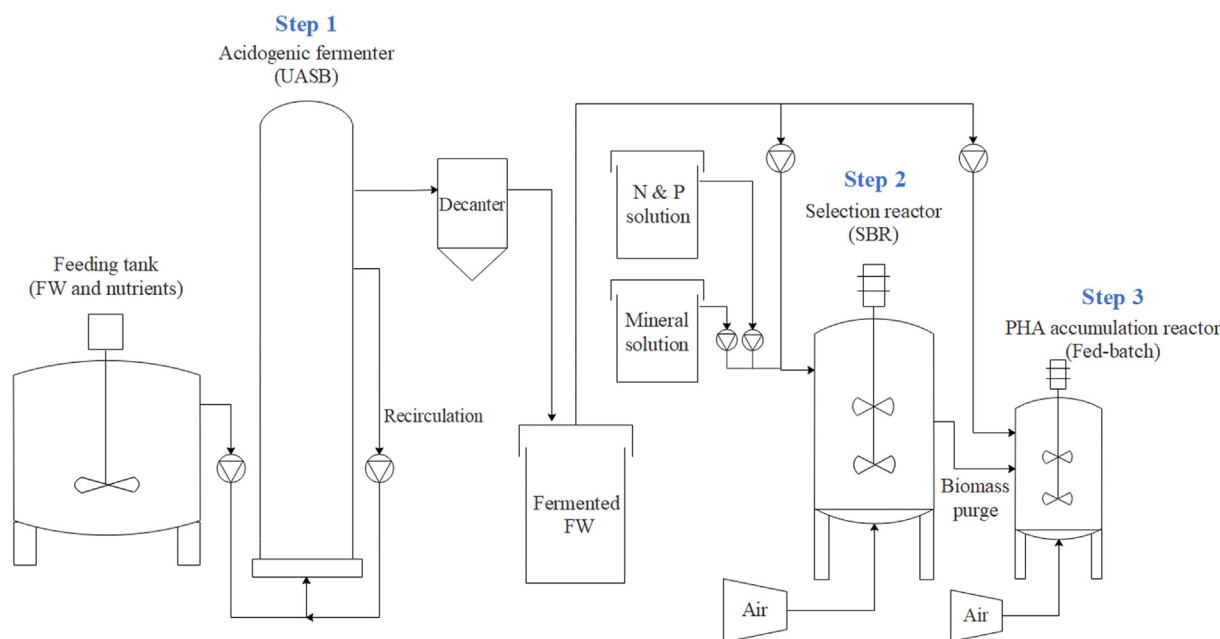


Fig. 1. Configuration of the pilot plant unit adopted in this study.

follows: temperature of 29.7 ± 0.7 °C, pH 5.0 ± 0.1 , HRT of 24 h and OLR of 30 ± 2 gCOD.L⁻¹.d⁻¹.

The FW feedstock (Sumol+Compal S.A., Portugal) had a high total chemical oxygen demand (175 ± 13 gCOD.L⁻¹) which was adjusted with tap water to achieve the desired OLR. The feedstock was comprised of $85\% \pm 1\%$ (gCOD basis) of soluble biodegradable compounds prior to fermentation, which were fully exhausted.

The characteristics of the clarified fermented stream used as feedstock for the selection and accumulation reactors are listed in Table 1. The stream was largely comprised of PHA bioprecursors, namely volatile fatty acids (VFAs)– acetate (HAce), propionate (HPro), butyrate (HBut) and valerate (HVal) – lactate (HLac) and ethanol (EtOH) (Reis et al., 2011). Additionally, it was nutrient-deficient (low ammonium and phosphate concentrations) enabling the implementation of an uncoupled C–N feeding strategy in the selection reactor.

2.1.2. Culture selection reactor

Two 100 L SBRs were inoculated with fresh activated sludge (Mutela WWTP, Portugal) and operated with a HRT of 1 d, at room temperature and under uncontrolled pH. The two SBRs were operated with different SRTs: 4 d in SBR 4d and 2 d in SBR 2d. Air was provided at $60 L_{air} \cdot L_{reactor}^{-1} \cdot h^{-1}$, which was sufficient to ensure a dissolved oxygen (DO) above $2 \text{ mg-O}_2 \cdot \text{L}^{-1}$ throughout the cycle, to guarantee non-limiting conditions.

The SBR cycles had a length of 12 h, comprising: influent feeding (0.20 h), aerated feast/famine period (10.88 h), biomass withdrawal (0.20 h, only once a day in the case of SBR 4d), settling (0.75 h) and

withdrawal of exhausted effluent (0.17 h). A solution containing ammonium and phosphate (N & P solution) was fed after 3 h or 4 h (SBR 4d or SBR 2d, respectively) of the beginning of the cycle in order to keep the N feeding uncoupled from the C. The C:N:P ratio was adjusted to 100:7:1 (mol-basis) (Silva et al., 2017).

The OLR was increased in four steps for both SBRs: 2.6, 5.4, 6.6, 9.3 and 12.3 gCOD.L⁻¹.d⁻¹ for the SBR 4d, and 2.7, 6.3, 10.6, 12.9 and 14.5 gCOD.L⁻¹.d⁻¹ for the SBR 2d. The clarified SFP stream was diluted using a mineral solution to adjust the reactor OLR to the desired values, as described by Serafim et al. (2004).

The SBRs working sequence (pump filling, aeration, mixing and withdrawal) was automatically controlled by a software developed within the research group, which also recorded in real time the values of DO and pH. The DO trends allowed to identify the length of the feast phase, which is a parameter used to easily assess the performance of the feast–famine regime. During the feast phase, the DO is low due to microbial consumption for substrate oxidation. At the end of the feast phase, a sharp increase in the DO concentration profile occurs indicating the depletion of the organic carbon thus corresponding to the start of the famine phase.

The profiles of total suspended solids (TSS), PHA content on biomass and available SFP, nitrogen and phosphorus were assessed for each OLR tested.

2.1.3. PHA accumulation fed-batch assays

The maximum storage capacity of the MMCs selected at the highest OLR values was assessed in fed-batch accumulation assays carried out in a 60 L reactor. The assays (performed in duplicate) consisted on feeding the SFP without nutrient supplementation to 25 L of biomass collected from each one of the SBRs at the end of famine phase. The reactor was operated at room temperature, oxygen was supplied by sparging air at $60 L_{air} \cdot L_{reactor}^{-1} \cdot h^{-1}$, and the pH was controlled at 8.5 by automatically adding the acid SFP stream (pH-stat mode).

2.2. Analytical methods

LCK 914 Hach Lange kits (Hach-Lange, Germany) were used to determine chemical oxygen demand (COD) following the manufacturer's instructions.

Table 1

Characteristics of the clarified fermented feedstock. Ranges of the key parameters are presented as minimum/maximum values detected in the feedstock.

| Parameter | Min/max values |
|---|-------------------------------|
| Ammonium (mg-N.L ⁻¹) | 0/9 |
| Phosphate (mg-P.L ⁻¹) | 11/32 |
| SFP concentration (gCOD.L ⁻¹) | 22/26 |
| SFP composition (% gCOD-basis) | HLac HAce HPro EtOH HBut HVal |
| | 0/2 15/31 3/13 0/9 51/68 2/12 |

TSS and volatile suspended solids (VSS) were determined using the protocol described in Standard Methods (APHA, 1998).

SFP concentrations of filtered samples were determined through high performance liquid chromatography (HPLC) using a VWR Hitachi Chromaster chromatographer as described by Oliveira et al. (2017).

Ammonium and phosphate concentrations were determined using a colorimetric method implemented in a segmented flow analyser (Skalar San++ system, Skalar Analytical).

Lyophilised biomass pellets were processed using the method described by Lanham et al. (2013) to quantify 3-hydroxybutyrate (3-HB) and 3-hydroxyvalerate (3-HV) monomer concentrations by gas chromatography (GC) using a Bruker 430-GC gas chromatographer.

Molecular mass distribution (M_w) and polydispersity indices (PDI) of the produced PHA were determined by size exclusion chromatography (SEC) (Waters Millennium system) as described by Pereira et al. (2019).

A detailed description of these methodologies can be found in Appendix A.

2.3. Microbiological analyses

Biomass samples were collected in both SBR 4d and SBR 2d throughout the operational period and were phylogenetically characterised based on high throughput sequencing of the 16S rRNA gene. DNA was extracted with the FastDNA Spin kit for soil (MP Biomedicals, USA), using the standard protocol with a few exceptions: sample of 500 μL , 480 μL of Sodium Phosphate Buffer and 120 μL of MT Buffer were added to a tube of Lysing Matrix. 16S rRNA gene amplicon sequencing and bioinformatic processing was carried out using Illumina technology by DNASense (Aalborg, Denmark).

Principal component analysis (PCA) was performed to visually detect the dynamics of the microbial communities throughout the study. Prior to the analysis, operational taxonomic units (OTUs) that are not present in more than 0.1% relative abundance were removed. The data was transformed by applying the Hellinger transformation (Legendre and Gallagher, 2001). The distance between the data points plotted is indicative of the similarity of the microbial composition of the samples.

Putative PHA-storers were identified using the references reported in Appendix C (Table C3).

2.4. Calculations

Feast to famine length ratio (FF ratio, $\text{h}\cdot\text{h}^{-1}$) was calculated as the fraction between the time lengths of the feast and the famine phases.

The percentages of PHA content in biomass (% w/w) were assessed by dividing the PHA content by the measured VSS determined at the same time of the assay. The active biomass (X_a , $\text{g}\cdot\text{L}^{-1}$) concentrations were calculated by the difference between VSS concentration ($\text{g}\cdot\text{L}^{-1}$) and PHA concentration ($\text{g}\cdot\text{L}^{-1}$) (at the same reaction time).

Biomass volumetric productivity (P_x) was calculated by the fraction between X_a concentration ($\text{g}\cdot\text{X}_a\cdot\text{L}^{-1}$) and the SRT (d).

Specific substrate uptake rates ($-q_{\text{SFP}}$, $\text{gCOD}\cdot\text{SFP}\cdot\text{gCOD}\cdot\text{X}_a^{-1}\cdot\text{L}^{-1}$), specific PHA storage (q_{PHA} , $\text{gCOD}\cdot\text{PHA}\cdot\text{gCOD}\cdot\text{X}_a^{-1}\cdot\text{h}^{-1}$) and consumption ($-q_{\text{PHA}}^{\text{famine}}$, $\text{gCOD}\cdot\text{PHA}\cdot\text{gCOD}\cdot\text{X}_a^{-1}\cdot\text{h}^{-1}$) rates, and maximum specific growth rates (μ_{max} , h^{-1}) were calculated from the slope of the linear regression of total SFP, PHA and X_a specific concentrations, respectively, over time. The goodness-of-fit of each linear regression was assessed by the R^2 ($R^2 > 0.80$).

Storage yields ($Y_{\text{PHA/SFP}}$, $\text{gCOD}\cdot\text{PHA}\cdot\text{gCOD}\cdot\text{SFP}^{-1}$) were calculated by dividing the q_{PHA} by the $-q_{\text{SFP}}$. Growth yields on PHA ($Y_{\text{X/PHA}}$, $\text{gCOD}\cdot\text{X}_a\cdot\text{gCOD}\cdot\text{PHA}^{-1}$) were determined as the ratio between μ_{max} and $-q_{\text{PHA}}^{\text{famine}}$.

Concentrations of all carbon compounds (3-HB, 3-HV, SFP and X_a) were converted into COD units in accordance with the oxidation stoichiometry presented in Appendix A.

3. Results

Two PHA-storing cultures were selected with SRT of either 4 d or 2 d and gradually increased OLR. The performance and population dynamics were evaluated in the SBR and through assays in the accumulation fed-batch reactor to characterise and compare the two cultures.

3.1. Culture selection

3.1.1. SRT of 4d

For the SBR operated at 4d of SRT (SBR 4d), the OLR was initially set to $2.60\text{ gCOD}\cdot\text{L}^{-1}\cdot\text{d}^{-1}$, then increased in four steps up to $12.3\text{ gCOD}\cdot\text{L}^{-1}\cdot\text{d}^{-1}$ (see Fig. B1 A in Appendix B for more details). The performance of the culture was assessed for each OLR tested, and the results are summarised in Table 2.

The observed FF ratio did not increase significantly along the operation period despite the increase in OLR (Fig. B1 A in Appendix B). In fact, the FF decreased after an initial value of 0.16 during start-up, and remained consistently below 0.1 during the rest of the operation period (Table 2). On the other hand, the increase of OLR had a high impact on the active biomass (X_a) concentration, which raised from 1.75 to $7.9\text{ g}\cdot\text{X}_a\cdot\text{L}^{-1}$.

The specific substrate uptake ($-q_{\text{SFP}}$) and storage (q_{PHA}) rates showed an unexpected trend. Both rates increased sharply with the OLR up to maximum values of $1.1\text{ gCOD}\cdot\text{gCOD}\cdot\text{X}_a^{-1}\cdot\text{h}^{-1}$ and $1.01\text{ gCOD}\cdot\text{gCOD}\cdot\text{X}_a^{-1}\cdot\text{h}^{-1}$, respectively, for an OLR of $6.6\text{ gCOD}\cdot\text{L}^{-1}\cdot\text{d}^{-1}$, while further increase of OLR to $12.3\text{ gCOD}\cdot\text{L}^{-1}\cdot\text{d}^{-1}$ caused a decrease to $0.55\text{ gCOD}\cdot\text{gCOD}\cdot\text{X}_a^{-1}\cdot\text{h}^{-1}$ and $0.41\text{ gCOD}\cdot\text{gCOD}\cdot\text{X}_a^{-1}\cdot\text{h}^{-1}$, respectively (Table 2). The same trend was observed for the storage yield ($Y_{\text{PHA/SFP}}$), which attained maximum values of $0.90\text{ gCOD}\cdot\text{gCOD}^{-1}$ at the middle-range OLRs ($5.4\text{--}6.6\text{ gCOD}\cdot\text{L}^{-1}\cdot\text{d}^{-1}$) and tended to decrease for higher OLR values (Table 2).

The performance parameters relative to the famine period (e.g. maximum specific PHA consumption ($-q_{\text{PHA}}^{\text{famine}}$), maximum growth rates (μ_{max}) and growth yield on PHA ($Y_{\text{X/PHA}}$) were relatively stable despite the increase in OLR, excluding the first OLR period which coincided with the acclimation period (Table 2).

The PHA obtained in the process throughout this experiment was a copolymer of 3-HB and 3-HV monomers, with a 3-HV content that varied between 14.0% and 24.6% on a Cmol-basis.

3.1.2. SRT 2d

Similarly to the SBR 4d, in the reactor operated at SRT of 2 d (SBR 2d) the OLR was initially set to $2.7\text{ gCOD}\cdot\text{L}^{-1}\cdot\text{d}^{-1}$ and increased in four steps up to $14.5\text{ gCOD}\cdot\text{L}^{-1}\cdot\text{d}^{-1}$ (see Fig. B1 B in Appendix B for more details). The results are summarised in Table 2.

The FF ratio varied slightly with the OLR increments, ranging between 0.24 and 0.39 in the stable periods (Table 2).

The X_a concentration increased linearly with the increasing OLR up to a value of $4.67\text{ g}\cdot\text{X}_a\cdot\text{L}^{-1}$ at the maximum OLR tested ($14.5\text{ gCOD}\cdot\text{L}^{-1}\cdot\text{d}^{-1}$) (Table 2).

The performance of this culture was quite different from that of the culture selected in SBR 4d. The $-q_{\text{SFP}}$ and q_{PHA} increased with the OLR reaching maximum values of $0.65\text{ gCOD}\cdot\text{gCOD}\cdot\text{X}_a^{-1}\cdot\text{h}^{-1}$ and $0.50\text{ gCOD}\cdot\text{gCOD}\cdot\text{X}_a^{-1}\cdot\text{h}^{-1}$, respectively, at OLR $14.5\text{ gCOD}\cdot\text{L}^{-1}\cdot\text{d}^{-1}$. Also, the $Y_{\text{PHA/SFP}}$ increased from $0.41\text{ gCOD}\cdot\text{gCOD}^{-1}$ to $0.77\text{ gCOD}\cdot\text{gCOD}^{-1}$. After the initial variations observed during the first OLR step, which were likely due to acclimatisation, no significant fluctuations were observed for the parameters determined during the famine period, such as the $-q_{\text{PHA}}^{\text{famine}}$, the μ_{max} and the $Y_{\text{X/PHA}}$ (Table 2).

The copolymer produced had a 3-HV content ranging between 10.8% and 23.2% (Cmol-basis) in this experiment.

3.2. PHA accumulation assays

The storage response of the cultures selected at the highest OLRs in each of the SBRs was evaluated in two fed-batch accumulation assays

Table 2Main parameters monitored and determined for SBR operation at SBR 4d and SBR 2d for each OLR tested. Values presented are **mean** (standard deviation).

| | SBR 4d | | | | | SBR 2d | | | | |
|--|-------------------------|-------------------------|-------------------------|-------------------------|-------------------------|-------------------------|-------------------------|-------------------------|-----------------------|-------------------------|
| OLR (gCOD.L ⁻¹ .d ⁻¹) | 2.60 (0.01) | 5.4 (0.1) | 6.6 (0.5) | 9.3 (0.1) | 12.3 (0.1) | 2.7 (0.2) | 6 (1) | 10.6 (0.5) | 12.9 (0.2) | 14.5 (0.6) |
| FF ratio (h.h ⁻¹) | 0.16 (0.009) | 0.056 (0.005) | 0.035 (0.005) | 0.056 (0.006) | 0.09 (0.01) | 0.30 (0.03) | 0.24 (0.01) | 0.35 (0.02) | 0.39 (0.03) | 0.27 (0.03) |
| X _a (g.L ⁻¹) | 1.75 (0.05) | 4.84 (0.02) | 5.09 (0.09) | 6.97 (0.06) | 7.9 (0.3) | 1.24 (0.05) | 2.5 (0.3) | 3.6 (0.2) | 4.2 (0.6) | 4.67 (0.06) |
| Δ PHA feast (%, w/w) | 22.4 (0.02) | 18.2 (0.3) | 19.6 (0.7) | 18.9 (0.1) | 22 (1) | 32 (3) | 24.2 (0.9) | 22.6 (0.5) | 27 (1) | 26 (3) |
| -q _{SFP} (gCOD.gCOD-X _a ⁻¹ .h ⁻¹) | 0.44 (0.01) | 1.04 (0.04) | 1.1 (0.1) | 0.75 (0.05) | 0.55 (0.07) | 0.45 (0.03) | 0.47 (0.05) | 0.52 (0.03) | 0.58 (0.03) | 0.65 (0.03) |
| q _{PHA} (gCOD.gCOD-X _a ⁻¹ .h ⁻¹) | 0.209 (0.005) | 0.93 (0.03) | 1.01 (0.05) | 0.61 (0.04) | 0.41 (0.07) | 0.18 (0.02) | 0.29 (0.01) | 0.34 (0.04) | 0.40 (0.02) | 0.50 (0.01) |
| Y _{PHA/SFP} (gCOD.gCOD ⁻¹) | 0.47 (0.02) | 0.90 (0.04) | 0.90 (0.09) | 0.81 (0.08) | 0.74 (0.02) | 0.41 (0.05) | 0.62 (0.04) | 0.66 (0.08) | 0.69 (0.06) | 0.77 (0.02) |
| -q _{PHA^{famine}} (gCOD.gCOD-X _a ⁻¹ .h ⁻¹) | 0.128 (0.006) | 0.07 (0.01) | 0.083 (0.002) | 0.063 (0.001) | 0.068 (0.006) | 0.122 (0.003) | 0.145 (0.003) | 0.12 (0.01) | 0.12 (0.01) | 0.141 (0.006) |
| μ _{max} (h ⁻¹) | 0.10 (0.01) | 0.047 (0.004) | 0.054 (0.008) | 0.042 (0.003) | 0.044 (0.003) | 0.103 (0.008) | 0.109 (0.004) | 0.087 (0.006) | 0.08 (0.01) | 0.103 (0.006) |
| Y _{X/PHA} (gCOD.gCOD ⁻¹) | 0.80 (0.06) | 0.7 (0.1) | 0.7 (0.1) | 0.67 (0.05) | 0.66 (0.05) | 0.84 (0.07) | 0.75 (0.01) | 0.74 (0.08) | 0.76 (0.01) | 0.73 (0.07) |

performed in duplicate in the accumulation reactor: the Acc 4d (inoculated with SBR 4d biomass) and the Acc 2d (with biomass from SBR 2d). The assays were performed with no N addition, thus no microbial growth was enabled. The concentration of SFP in the reactor (C_{SFP}) was quite stable in the period when the specific rates and yields were calculated (3.80 ± 0.04 gCOD.L⁻¹ and 4.43 ± 0.07 gCOD.L⁻¹ for Acc 4d and Acc 2d, respectively (Table 3)). The supply of external carbon was practically continuous due to the operation with pH-stat control using the SFP solution to correct the pH. Due to this, no polymer was consumed during the accumulation assays. Both cultures were fed and aerated until a stable PHA content was attained, corresponding to their maximum PHA accumulation capacity.

Table 3 summarises the average maximum specific substrate uptake (-q_{SFP}) and storage (q_{PHA}) rates, storage yields (Y_{PHA/SFP}) and PHA content on biomass and the PHA characteristics obtained for the different assays.

In general, the storage response of the Acc 2d was lower than that observed in the Acc 4d. Despite the similar Y_{PHA/SFP}, the culture selected

Table 3Main parameters determined in the accumulation reactor inoculated with culture selected at the maximum OLR tested in SBR 4d (Acc 4d) and SBR 2d (Acc 2d). Values presented are **mean** (standard deviation).

| Reactor | Acc 4d | Acc 2d |
|--|---|---|
| Inoculum source | SBR 4d | SBR 2d |
| Culture selected at OLR (gCOD.L ⁻¹ .d ⁻¹) | 12.3 (0.1) | 14.5 (0.6) |
| C _{SFP} ^a (gCOD.L ⁻¹) | 3.80 (0.04) | 4.43 (0.07) |
| SFP composition [HLac/HAc/HPro/EtOH/HBut/HVal] (%, gCOD-basis) | 0/23.7/8.4/6/57.6/4.0 (0/0.2/0.2/1/0.2/0.7) | 0/19/3.9/7.8/67/2.2 (0/2/0.3/0.4/1/0.6) |
| -q _{SFP} ^b (gCOD.gCOD-X _a ⁻¹ .h ⁻¹) | 1.31 (0.09) | 0.6939 (0.0004) |
| q _{PHA} ^b (gCOD.gCOD-X _a ⁻¹ .h ⁻¹) | 0.97 (0.04) | 0.53 (0.03) |
| Y _{PHA/SFP} ^b (gCOD.gCOD ⁻¹) | 0.74 (0.02) | 0.76 (0.05) |
| Max. PHA content (%, w/w) | 69 (2) | 49.2 (0.4) |
| Polymer 3-HV content (%, w/w) | 16.8 (0.8) | 13.21 (0.02) |
| Polymer M _w (kDa) | 451 | 453 |
| Polymer PDI | 2.38 | 2.47 |

^a Average SFP concentration on reactor at the period where the specific rates and yield were calculated.

^b Maximum values.

at the lower SRT was only capable to accumulate a maximum amount of $49.2 \pm 0.4\%$ (w/w) of PHA, contrasting with the $69 \pm 2\%$ (w/w) obtained for SBR 4d biomass. In addition, the specific storage rate in Acc 2d (0.53 gCOD.gCOD-X_a⁻¹.h⁻¹) was nearly half of that observed in Acc 4d (0.97 gCOD.gCOD-X_a⁻¹.h⁻¹) (Table 3). This difference in performance by the two cultures contrasted with the behaviour observed in the SBRs (in the phase of maximum OLR), where the cultures had similar q_{PHA} (0.41 and 0.50 gCOD.gCOD-X_a⁻¹.h⁻¹ respectively for SBR 4d and SBR 2d) and Y_{PHA/SFP} (0.74 and 0.76 gCOD.gCOD⁻¹ respectively for SBR 4d and SBR 2d).

The polymer produced during the accumulation assays had a 3-HV fraction of $16.8 \pm 0.8\%$ and $13.21 \pm 0.02\%$ (w/w), for the cultures enriched with SRT of 4d and 2d, respectively, both of them displaying similar molecular weights (M_w) and polydispersity indices (PDI) (Table 3).

3.3. Microbial community analysis

Biomass samples collected at different OLRs (6.6 and 12.3 gCOD.L⁻¹.d⁻¹ from SBR 4d and 6.3, 12.9 and 14.5 gCOD.L⁻¹.d⁻¹ from SBR 2d) were analysed through high throughput sequencing of the 16S rRNA gene, and compared with the profile of the full-scale activated sludge used as inoculum.

Despite the similarity of the inoculum, the community enriched in the SBR 2d highly diverged from the one obtained in the SBR 4d, as evidenced by their distance in the PCA plot (Fig. 2). Additionally, the microbial profile clearly changed with the increase in OLRs in each of the reactors, as can be observed by the distances of the corresponding points in the PCA results (Fig. 2). Detailed high throughput sequencing results obtained for the SBR 2d and SBR 4d are presented, respectively, in Tables C1 and C2 in Appendix C. In the SBR 2d culture, the putative PHA-accumulating organisms consistently increased with the OLR, achieving 71.8% for the highest OLR. In contrast, a maximum relative abundance of putative PHA-storers of 93.0% was detected for the SBR 4d enrichment when operated at 6.6 gCOD.L⁻¹.d⁻¹. This value decreased to 60.0% at the maximum OLR but the putative PHA-storers concentration remained stable thereafter (Table 4), suggesting that above 6.6 gCOD.L⁻¹.d⁻¹ the increase of X_a reflected growth of flanking microorganisms.

4. Discussion

4.1. Growth vs storage response

The determined specific rates and yields were very similar between the two SBRs for the first OLR tested (Table 2). This similarity in the

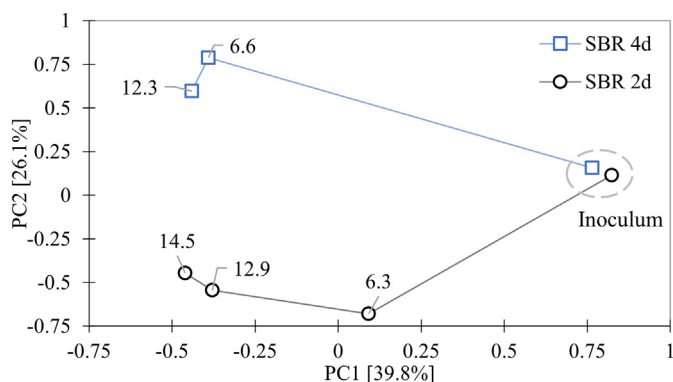


Fig. 2. PCA ordination highlighting the differences in OTUs abundance between the microbial communities selected in SBR 4d and SBR 2d (data labels correspond to the operational OLR). The relative contribution (eigenvalue) of each axis to the total inertia in the data is indicated in percent at the axis titles.

culture response can be attributed to the short period of acclimatisation time at this point (Fig. B1 in Appendix B), which is unlikely to be enough to enrich a PHA-storing community. For this reason, and considering that both reactors showed distinct yields and kinetic profiles throughout the rest of the study (Table 2), the parameters calculated for this initial operational period were not used as a mean of comparison between the assays.

The maximum specific growth rate (μ_{\max}), calculated during famine, was not affected by the OLR. As expected, the μ_{\max} was driven by the SRT, being 2.1 times higher, on average, for SBR 2d than for SBR 4d (Table 2). The same trend was observed for the $-q_{\text{PHA}}^{\text{famine}}$, which was the double for the SBR 2d than for the SBR 4d. The similar proportion in μ_{\max} and $-q_{\text{PHA}}^{\text{famine}}$ for SRT 4d and SRT 2d confirms that, in the famine phase, PHA and growth are fully correlated. The $Y_{\text{X/PHA}}$ were also not significantly different between OLR values for each SBR. However, these values were on average 15% higher for the SBR 2d than for the SBR 4d (see Table 2), indicating that when the uncoupled strategy is used, cultures selected at a lower SRT can use the accumulated PHA for growth more efficiently, independently of the OLR applied. Contrasting to what happens when using the traditional coupled feeding approach, the OLR did not affect the culture growth performance. In fact, in the traditional approach, growth and storage metabolisms compete with each other for the external substrate concentration (which is usually directly linked to the OLR) while in the uncoupled feeding the biomass grows from the stored PHA. Thus, in this case, if the culture is able to accumulate enough polymer to ensure unlimiting conditions, the OLR will have a low impact on the growth rate. The fact that, for the same SRT, the $-q_{\text{PHA}}^{\text{famine}}$ was constant for all the OLR tested, confirms that assumption.

Table 4

Relative abundance (% of total reads) and concentration of putative PHA-storers calculated for the cultures present in SBR 4d and SBR 2d. Values of putative PHA-storers concentration are mean (standard deviation).

| Reactor | OLR (gCOD.L ⁻¹ .d ⁻¹) | Relative abundance of putative PHA-storers (% of total reads) ^a | Concentration of putative PHA-storers (g.L ⁻¹) ^b |
|---------|--|--|---|
| SBR 4d | Inoculum | 18.9 | |
| | 6.6 | 93.3 | 4.8 (0.1) |
| | 12.3 | 60.2 | 4.8 (0.2) |
| SBR 2d | Inoculum | 12.3 | |
| | 6.3 | 21.9 | 0.55 (0.07) |
| | 12.9 | 47.4 | 2.0 (0.3) |
| | 14.5 | 71.8 | 3.36 (0.04) |

^a According to the relative abundance of sequences affiliated with known putative PHA-storers (more details can be found in Appendix C).

^b Estimated using the corresponding X_{a} presented in Table 2.

The $Y_{\text{PHA/SFP}}$ followed different trends in the two SBRs as the OLR was increased, tending to decrease in SBR 4d and to increase in SBR 2d (Fig. 3 A). It was hypothesised that those differences in the $Y_{\text{PHA/SFP}}$ could be related with the abundance of PHA-storing bacteria selected at each condition. In fact, as shown in Fig. 3 B, the $Y_{\text{PHA/SFP}}$ trends seem to be directly related with the enrichment of the culture in putative PHA-storers indicating that, independently of the OLR and SRT, an efficient microbial selection seems to be the driving force to obtain a high storage yield. If a deeper characterization of the microbial population is required, it is recommended to analyse the PHA synthase gene to effectively determine the abundance of PHA-storing organisms and validate this hypothesis.

The genus *Paracoccus* significantly dominated the MMC at SBR 4d (see Table C1 in Appendix C), however as the OLR increased beyond 6.6 gCOD.L⁻¹.d⁻¹ a sudden decrease in the abundance of *Paracoccus* was observed. *Paracoccus* growth has previously been reported to be potential inhibited by high OLR values (Wen et al., 2018), which may have happened in this case. Additionally, a substrate inhibition period observed at this phase (as further discussed below) may have given the opportunity of flanking populations to thrive, making the relative abundance of putative PHA-storers to significantly decrease from the 93.3% to 60.2% at the maximum OLR (Table 4). For the SBR 2d the increasing OLR favoured the growth of other putative PHA-storers, which may not have been as susceptible to substrate inhibition (Table 4).

The highest relative abundance of putative PHA-storers (93.3%) and high storage yield (0.90 gCOD.gCOD⁻¹) were observed for the SBR 4d operated at 6.6 gCOD.L⁻¹.d⁻¹ (Fig. 3 B). This value was quite high when compared with studies where the coupled feeding approach was used. For example, Moretto et al. (2020), who studied the effect of SRT using the coupled strategy, obtained a maximum abundance of putative PHA-storers of only 64% using an SRT of 1 d and an OLR of 4.0 gCOD.L⁻¹.d⁻¹. This demonstrates that, as expected, the uncoupled strategy in this study worked as an effective measure to increase the selective pressure to enrich for PHA-accumulating organisms.

In the current work, the two C-uptake mechanisms (storage and growth) are separated and use different carbon sources (SFP and stored PHA, respectively), thus the $Y_{\text{PHA/SFP}}$ was maximal for each operating condition and was only dependent on the relative abundance of putative PHA-storers. This response differs from the cultures fed with the coupled strategy in which $Y_{\text{PHA/SFP}}$ is conditioned by either the PHA-storers abundance or the growth kinetics. For instance, in SBR 4d at OLR 12.3 gCOD.L⁻¹.h⁻¹, 60.2% of the enriched community was comprised of putative PHA-storers (Table 4), a value that was very similar to that obtained by Moretto et al. (2020) for their best-case scenario (64% of putative PHA-storers for an SRT of 1 d and OLR of 4.0 gCOD.L⁻¹.d⁻¹). However, the $Y_{\text{PHA/SFP}}$ obtained in the current study was substantially higher (0.74 gCOD.gCOD⁻¹, Table 2, vs 0.46 gCOD.gCOD⁻¹, Moretto et al. (2020)), likely because in the latter study, growth and storage occurred simultaneously at the expense of the external carbon feed, decreasing its availability for storage.

The storage rates trends were also highly affected by the OLR (Fig. 4 A). The q_{PHA} in SBR 4d were initially more than 3-fold higher than in SBR 2d, although from OLR 6.6 gCOD.L⁻¹.d⁻¹ onwards the q_{PHA} tended to decrease in the SBR 4d and to increase in SBR 2d, converging to similar values (Fig. 4 A).

The decreased q_{PHA} observed in SBR 4d seemed to be a clear consequence of substrate inhibition rather than the result of culture selection. This hypothesis is validated by the results obtained in the accumulation reactor Acc 4d (Fig. 4 B), in which a lower SFP concentration was applied (SFP in the reactor of 3.80 gCOD.L⁻¹, Table 3), similar to the one imposed when the maximum q_{PHA} was observed (OLR 6.6 gCOD.L⁻¹.d⁻¹, which corresponds to a SFP concentration in the reactor of 3.3 gCOD.L⁻¹). It was found that the SBR 4d culture selected at OLR 12.3 gCOD.L⁻¹.d⁻¹, and then used as inoculum in Acc 4d, showed a q_{PHA} value similar to that maximum obtained for the OLR 6.6 gCOD.L⁻¹.d⁻¹ (Fig. 4 A – orange rectangle). This result indicates that higher q_{PHA} could also be

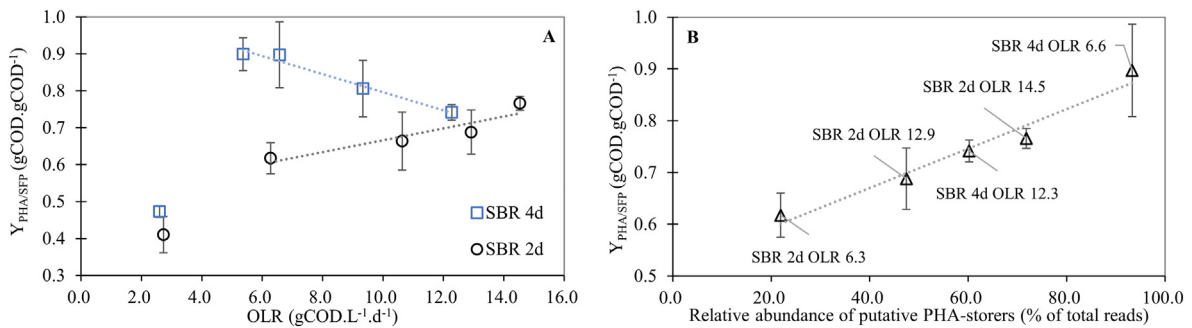


Fig. 3. Storage yields ($Y_{PHA/SFP}$) as a function of (A) the different OLR values applied and (B) the relative abundance of known putative PHA-storers, determined in the SBR 4d and SBR 2d.

achieved by the culture selected at the maximum OLR when no substrate inhibition conditions are applied, as occurred in Acc 4d.

Interestingly, the inhibition effect was not observed for the SBR 2d. As shown in Fig. 4 A (yellow rectangle), the culture selected at the maximum OLR in SBR 2d showed similar q_{PHA} values when inoculated in Acc 2d at a lower SFP concentrations (7.25 gCOD.L⁻¹ in SBR 2d and 4.43 gCOD.L⁻¹ in Acc 2d – Table 3). Additionally, the q_{PHA} increased with the OLR throughout the whole experiment, suggesting that, when using the uncoupled strategy, cultures selected at lower SRT are less sensitive to high SFP concentrations. In sum, comparing the real q_{PHA} (i.e., when no substrate inhibition is observed) of the cultures selected at the different SRTs it is possible to conclude that, regardless of the amount of putative PHA-accumulators, the cultures selected at the highest SRT (SBR 4d) had faster intrinsic storage kinetics at all OLRs tested (Fig. 4 B).

When the coupled feeding strategy is used, the growth kinetics of a PHA-producing MMC is favoured at lower SRT for both carbon and nitrogen limited cultures. However, the cultures selected under nitrogen limited conditions always showed higher ammonia uptake rates than the carbon limited ones, independently on the SRT used (Johnson et al., 2010). Regarding the storage mechanism, Johnson et al. (2010) did not report detailed measurements on the specific storage rates obtained in the accumulation assays. Thus, no clear correlation was made between the operating condition imposed in the SBR (different SRT and/or type of limitation) and the intrinsic storage kinetics of the culture (i.e., when the selected MMC is subjected to C excess under nutrient-limiting conditions to ensure no competition between growth and storage). From the best of the authors knowledge, there are no other studies in the literature that allow to infer about the relationship between the culture intrinsic growth and storage behaviour and the selection SRT. Lemos et al. (2008) studied the SRT on nitrogen-limited cultures but also did not reported detailed data of accumulation assays. On the other hand, Chen et al. (2017) reported the accumulation measurements, but did not specify the type of limitation at which the cultures

were being selected, making impossible to compare their growth behaviour. Lastly, Moretto et al. (2020) also did not show the type of selection limitation and neither kinetic results obtained in accumulation assays under nutrient-limiting conditions.

When operating under the uncoupled feeding approach, there is no competition between the growth and storage mechanism. Thus, it can be assumed that the culture growth and storage intrinsic responses are driven only by the applied SRT, which physically selects PHA-storers with distinct abilities. Higher SRTs favoured the growth of organisms that have a high affinity towards the external substrate and faster storage kinetics. In contrast, applying a lower SRT favoured the selection of populations which are characterised by having higher maximum specific growth rates and lower storage rates.

4.2. Impact of the operational conditions on PHA production process

The physicochemical properties of PHA are highly influenced by the monomeric composition and M_w (Lorini et al., 2020b; Philip et al., 2007). In current work, the polymer 3-HV monomeric production varied linearly with the fraction of 3-HV precursors (propionate and valerate) in the feed, for all the SBR and accumulation assays (see Fig. D1 in Appendix D). Additionally, no significant differences were observed within the linear correlations obtained for the two cultures selected at the different SRTs (Fig. D1 in Appendix D), and the polymers obtained in the accumulation assays had similar M_w and PDI (Table 3) indicating that similar polymers can be produced with different selected cultures. The M_w observed (451 and 453 kDa, respectively for the polymers produced in Acc 4d and Acc 2d) was in the same order of magnitude than those reported in previous studies for commercial PHA produced from pure cultures (200–660 kDa) and for PHA produced from MMCs and waste-based feedstocks (220–650 kDa) (Albuquerque et al., 2011; Duque et al., 2014; Lorini et al., 2020b). A polymer with a M_w higher than 400 kDa and with a 3-HV monomeric composition between 7% and 20% (w/w), which was the case of the polymers obtained within

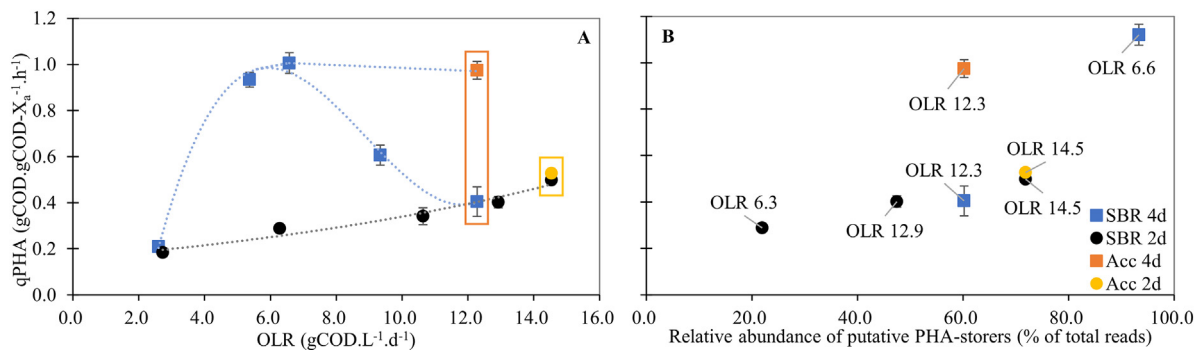


Fig. 4. Specific storage rates (q_{PHA}) obtained in the SBRs and accumulation assays as a function of (A) the different OLR values applied in SBRs and (B) the relative abundance of known putative PHA-storers of the cultures selected at the different OLRs in SBR 4d and SBR 2d. The orange and yellow rectangles highlight q_{PHA} obtained for the same culture inoculated in the SBR and Acc reactors.

this work, is considered to have good mechanical properties, lower melting temperature, increased flexibility and enhanced gas barrier properties when compared with pure PHB, making it suitable e.g. for food packaging applications (Lorini et al., 2020b; Philip et al., 2007).

The global productivity of the PHA process can be used as indicator of overall performance. It can be calculated considering the biomass volumetric productivity (P_X) in the SBR and the maximum culture accumulation capacity in accumulation assays, thus reflecting the balance achieved between the growth and storage response. As expected, the P_X evolution was very responsive to the OLR in both SBR 4d and SBR 2d. For each OLR, the SRT did not impact the biomass productivity (Fig. 5).

On the other hand, despite the higher relative abundance of putative PHA-storers in SBR 2d at the maximum OLR tested (Table 4), this culture had inferior PHA accumulation capacity. At the end of the Acc 2d, the MMC was only capable to accumulate a maximum amount of $49.2 \pm 0.4\%$ (w/w) of PHA, contrasting with the $69 \pm 2\%$ (w/w) obtained for Acc 4d (Table 3). This behaviour seemed to be an intrinsic limitation associated to the microbial composition, confirming that, in fact, the culture selected in SBR 2d had a lower storage capability than the one selected at 4 d of SRT. Although the P_X was similar for both cultures, the superior accumulation capability of the culture selected at SRT 4 d greatly increased the global PHA productivity, which was almost 80% higher for the SBR 4d culture ($4.6 \pm 0.3 \text{ g.L}^{-1}.\text{d}^{-1}$) than for SBR 2d ($2.6 \pm 0.2 \text{ g.L}^{-1}.\text{d}^{-1}$). The process productivity has a high impact on the operating and investment costs, therefore it can be anticipated that the final PHA manufacturing cost will be lower for the higher SRT, demonstrating the potential of using the SRT in combination with OLR as tuning design parameters to increase the MMC PHA-process viability. Lorini et al. (2020a) operated a SBR system similar to the SBR 4d in this study in terms of OLR ($12.725 \text{ gCOD.L}^{-1}.\text{d}^{-1}$) and C, N feeding strategy, although at different SRT (1 d). This study reported a PHA productivity of $2.4 \pm 0.1 \text{ g.L}^{-1}.\text{d}^{-1}$ as a result of the lower PHA accumulation capacity of the culture ($53 \pm 3\%$, w/w), which may have been a consequence of the low SRT imposed.

It should also be noted that a period of substrate inhibition in SBR 4d may have affected the selection of PHA-storers. So it can be hypothesised that, if this substrate inhibition could have been avoided, thus maintaining the PHA-storers relative abundance, an even higher global PHA productivity could have been reached using the SRT of 4d and the high OLR tested. To avoid this substrate inhibition, continuous or fed batch SBR feeding should be studied in order to assess the consequent impact on the overall process performance (maximum accumulation capacity and global storage yield and productivity).

The work herein discussed underlines the importance of in-depth understanding the impact of the SRT and OLR on the culture performance (growth/storage kinetics and accumulation capacity) to further optimising the PHA production process increasing its viability.

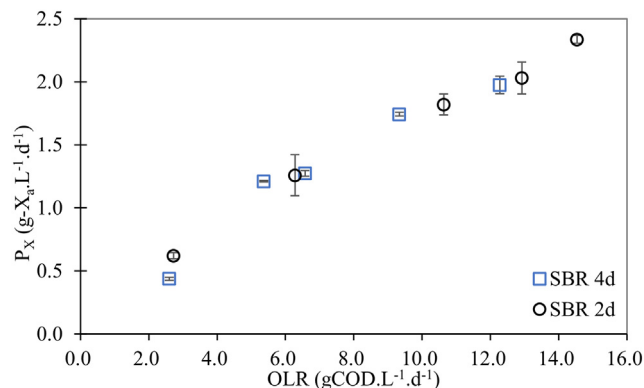


Fig. 5. Influence of the OLR values in the biomass volumetric productivity (P_X) obtained for the SBR 4d and SBR 2d.

5. Conclusions and prospects

This work assesses, for the first time, the impact of the SRT and the OLR on the growth and storage dynamics of PHA-storers selected under uncoupled C and N availabilities.

The OLR works essentially as a means to increase the biomass productivity, which is similar for each OLR regardless the SRT. A maximum biomass productivity of $2.3 \text{ g-X}_a.\text{L}^{-1}.\text{d}^{-1}$ was achieved in this study. Both tested SRTs seemed to result in highly enriched PHA-accumulating cultures but the higher-SRT culture was more easily inhibited by high substrate concentrations. However, this culture had faster storage kinetics (83% faster) and enhanced accumulation capacity (40% higher), resulting in a global PHA productivity almost 80% above that observed for the lower-SRT community.

The study herein presented opens the possibility of, when using a nutrient-deficient substrate that allows the implementation of an uncoupled feeding strategy, maximising the process performance by tuning the SRT of the selection reactor in combination with the OLR applied.

Supplementary data to this article can be found online at <https://doi.org/10.1016/j.scitotenv.2021.149363>.

CRediT authorship contribution statement

Mariana Matos: Conceptualization, Methodology, Investigation, Visualization, Writing – original draft. **Rafaela A.P. Cruz:** Methodology, Investigation. **Pedro Cardoso:** Investigation. **Fernando Silva:** Investigation. **Elisabete B. Freitas:** Investigation. **Gilda Carvalho:** Conceptualization, Writing – review & editing. **Maria A.M. Reis:** Supervision, Funding acquisition, Conceptualization, Writing – review & editing.

Declaration of competing interest

The authors declare that they have no known competing financial interests or personal relationships that could have appeared to influence the work reported in this paper.

Acknowledgments

Mariana Matos acknowledge FCT for PhD Grant SFRH/BD/104767/2014. This work was financially supported by the European Union's Horizon 2020 research and innovation program (GA 773375) and by UCIBIO (financed by FCT, UIDP/04378/2020 and UIDB/04378/2020).

References

- Albuquerque, M.G.E., Eiroa, M., Torres, C., Nunes, B.R., Reis, M.A.M., 2007. Strategies for the development of a side stream process for polyhydroxyalkanoate (PHA) production from sugar cane molasses. *J. Biotechnol.* 130, 411–421. <https://doi.org/10.1016/j.jbiotec.2007.05.011>.
- Albuquerque, M.G.E., Martino, V., Pollet, E., Avérous, L., Reis, M.A.M., 2011. Mixed culture polyhydroxyalkanoate (PHA) production from volatile fatty acid (VFA)-rich streams: effect of substrate composition and feeding regime on PHA productivity, composition and properties. *J. Biotechnol.* <https://doi.org/10.1016/j.jbiotec.2010.10.070>.
- APHA, 1998. *Standard Methods for Examination of Water and Wastewater*. 20th ed. American Public Health Association, Washington, DC.
- Argiz, L., González-Cabaleiro, R., Val del Río, Á., González-López, J., Mosquera-Corral, A., 2021. A novel strategy for triacylglycerides and polyhydroxyalkanoates production using waste lipids. *Sci. Total Environ.* 763, 142944. <https://doi.org/10.1016/j.scitotenv.2020.142944>.
- Campanari, S., Augelletti, F., Rossetti, S., Sciubba, F., Villano, M., Majone, M., 2017. Enhancing a multi-stage process for olive oil mill wastewater valorization towards polyhydroxyalkanoates and biogas production. *Chem. Eng. J.* 317, 280–289. <https://doi.org/10.1016/j.cej.2017.02.094>.
- Chen, Z., Huang, L., Wen, Q., Zhang, H., Guo, Z., 2017. Effects of sludge retention time, carbon and initial biomass concentrations on selection process: from activated sludge to polyhydroxyalkanoate accumulating cultures. *J. Environ. Sci. (China)* 52, 76–84. <https://doi.org/10.1016/j.jes.2016.03.014>.
- De Donno Novelli, L., Moreno Sayavedra, S., Rene, E.R., 2021. Polyhydroxyalkanoate (PHA) production via resource recovery from industrial waste streams: a review of

- techniques and perspectives. *Bioresour. Technol.* 331, 124985. <https://doi.org/10.1016/j.biortech.2021.124985>.
- Duque, A.F., Oliveira, C.S.S., Carmo, I.T.D., Gouveia, A.R., Pardelha, F., Ramos, A.M., Reis, M.A.M., 2014. Response of a three-stage process for PHA production by mixed microbial cultures to feedstock shift: impact on polymer composition. *New Biotechnol.* 31, 276–288. <https://doi.org/10.1016/j.nbt.2013.10.010>.
- European Bioplastics, 2020. Bioplastics market data [WWW document]. URL <https://www.european-bioplastics.org/market/> (accessed 5.7.21).
- Geyer, R., Jambeck, J.R., Law, K.L., 2017. Production, use, and fate of all plastics ever made. *Sci. Adv.* 3, e1700782. <https://doi.org/10.1126/sciadv.1700782>.
- Johnson, K., Kleerebezem, R., van Loosdrecht, M.C.M., 2010. Influence of the C/N ratio on the performance of polyhydroxybutyrate (PHB) producing sequencing batch reactors at short SRTs. *Water Res.* <https://doi.org/10.1016/j.watres.2009.12.031>.
- Kumar, M., Ghosh, P., Khosla, K., Thakur, I.S., 2018. Recovery of polyhydroxyalkanoates from municipal secondary wastewater sludge. *Bioresour. Technol.* 255, 111–115. <https://doi.org/10.1016/j.biortech.2018.01.031>.
- Kumar, M., Rathour, R., Singh, R., Sun, Y., Pandey, A., Gnansounou, E., Andrew Lin, K.-Y., Tsang, D.C.W., Thakur, I.S., 2020. Bacterial polyhydroxyalkanoates: opportunities, challenges, and prospects. *J. Clean. Prod.* 263, 121500. <https://doi.org/10.1016/j.jclepro.2020.121500>.
- Lanham, A.B., Ricardo, A.R., Albuquerque, M.G.E., Pardelha, F., Carnevalha, M., Coma, M., Fradinho, J., Carvalho, G., Oehmen, A., Reis, M.A.M., 2013. Determination of the extraction kinetics for the quantification of polyhydroxyalkanoate monomers in mixed microbial systems. *Process Biochem.* <https://doi.org/10.1016/j.procbio.2013.07.023>.
- Legendre, P., Gallagher, E.D., 2001. Ecologically meaningful transformations for ordination of species data. *Oecologia* <https://doi.org/10.1007/s004420100716>.
- Lemos, P.C., Levantesi, C., Serafim, L.S., Rossetti, S., Reis, M.A.M., Tandoi, V., 2008. Microbial characterisation of polyhydroxyalkanoates storing populations selected under different operating conditions using a cell-sorting RT-PCR approach. *Appl. Microbiol. Biotechnol.* <https://doi.org/10.1007/s00253-007-1301-5>.
- Lorini, L., di Re, F., Majone, M., Valentino, F., 2020a. High rate selection of PHA accumulating mixed cultures in sequencing batch reactors with uncoupled carbon and nitrogen feeding. *New Biotechnol.* <https://doi.org/10.1016/j.nbt.2020.01.006>.
- Lorini, L., Martinelli, A., Pavan, P., Majone, M., Valentino, F., 2020b. Downstream processing and characterization of polyhydroxyalkanoates (PHAs) produced by mixed microbial culture (MMC) and organic urban waste as substrate. *Biomass Convers. Biorefinery* <https://doi.org/10.1007/s13399-020-00788-w>.
- Mannina, G., Presti, D., Montiel-Jarillo, G., Carrera, J., Suárez-Ojeda, M.E., 2020. Recovery of polyhydroxyalkanoates (PHAs) from wastewater: a review. *Bioresour. Technol.* 297, 122478. <https://doi.org/10.1016/j.biortech.2019.122478>.
- Markets and Markets, 2021. Polyhydroxyalkanoate (PHA) market by type (short chain length, medium chain length), production method (sugar fermentation, vegetable oil fermentation, methane fermentation), application, and region - global forecast to 2025 [WWW document]. URL <https://www.marketsandmarkets.com/Market-Reports/pha-market-395.html> (accessed 4.29.21).
- Moretto, G., Lorini, L., Pavan, P., Crognale, S., Tonanzi, B., Rossetti, S., Majone, M., Valentino, F., 2020. Biopolymers from urban organic waste: influence of the solid retention time to cycle length ratio in the enrichment of a Mixed Microbial Culture (MMC). *ACS Sustain. Chem. Eng.* <https://doi.org/10.1021/acsschemeng.0c04980>.
- Oliveira, C.S.S., Silva, C.E., Carvalho, G., Reis, M.A., 2017. Strategies for efficiently selecting PHA producing mixed microbial cultures using complex feedstocks: feast and famine regime and uncoupled carbon and nitrogen availabilities. *New Biotechnol.* 37, 69–79. <https://doi.org/10.1016/j.nbt.2016.10.008>.
- Pereira, J.R., Araújo, D., Marques, A.C., Neves, L.A., Grandfils, C., Sevrin, C., Alves, V.D., Fortunato, E., Reis, M.A.M., Freitas, F., 2019. Demonstration of the adhesive properties of the medium-chain-length polyhydroxyalkanoate produced by *Pseudomonas chlororaphis* subsp. *aurantiaca* from glycerol. *Int. J. Biol. Macromol.* <https://doi.org/10.1016/j.ijbiomac.2018.09.064>.
- Philip, S., Keshavarz, T., Roy, I., 2007. Polyhydroxyalkanoates: biodegradable polymers with a range of applications. *J. Chem. Technol. Biotechnol.* <https://doi.org/10.1002/jctb.1667>.
- Plastics Europe, 2020. Plastics – the facts 2020 [WWW document]. URL <https://www.plasticseurope.org/en/resources/publications/4312-plastics-facts-2020> (accessed 5.7.21).
- Reis, M., Albuquerque, M., Villano, M., Majone, M., 2011. Mixed culture processes for polyhydroxyalkanoate production from agro-industrial surplus/wastes as feedstocks. *Comprehensive Biotechnology*, Second Edition, Second Ed. Elsevier B.V. <https://doi.org/10.1016/B978-0-08-088504-9.00464-5>.
- Sabapathy, P.C., Devaraj, S., Meixner, K., Anburajan, P., Kathirvel, P., Ravikumar, Y., Zayed, H.M., Qi, X., 2020. Recent developments in polyhydroxyalkanoates (PHAs) production – a review. *Bioresour. Technol.* 306, 123132. <https://doi.org/10.1016/j.biortech.2020.123132>.
- Serafim, L.S., Lemos, P.C., Oliveira, R., Reis, M.A.M., 2004. Optimization of polyhydroxybutyrate production by mixed cultures submitted to aerobic dynamic feeding conditions. *Biotechnol. Bioeng.* 87, 145–160. <https://doi.org/10.1002/bit.20085>.
- Silva, F., Campanari, S., Matteo, S., Valentino, F., Majone, M., Villano, M., 2017. Impact of nitrogen feeding regulation on polyhydroxyalkanoates production by mixed microbial cultures. *New Biotechnol.* <https://doi.org/10.1016/j.nbt.2016.07.013>.
- Valentino, F., Morgan-Sagastume, F., Campanari, S., Villano, M., Werker, A., Majone, M., 2017. Carbon recovery from wastewater through bioconversion into biodegradable polymers. *New Biotechnol.* 37, 9–23. <https://doi.org/10.1016/j.nbt.2016.05.007>.
- Wen, Q., Ji, Y., Hao, Y., Huang, L., Chen, Z., Sposob, M., 2018. Effect of sodium chloride on polyhydroxyalkanoate production from food waste fermentation leachate under different organic loading rate. *Bioresour. Technol.* <https://doi.org/10.1016/j.biortech.2018.07.036>.